



INVESTIGATION ON IMPACT STRENGTH OF ADDITIVE MANUFACTURED BIOMIMETIC STRUCTURE

¹Shivam Singh, ²DR. Aravind Raj S,

¹Student, ²Associate Professor,

¹Department of manufacturing engineering,

¹Vellore institute of technology, Vellore Tamil Nadu India

ABSTRACT

Additive manufacturing emerged as the innovation in the manufacturing field. FDM is one of the AM technique in which polymer is used as filament and part is formed layer by layer as fuse deposition modeling. With the help of 3d printing used to manufacture complicated structures. Structures like bio-mimic, which have complicated designs, can be formed with Additive manufacturing techniques. Gyroid structure is an example of a biomimetic structure that is found in the wings of butterflies and on arctic flowers is basically a porous lattice structure also known as TPMS (Triply periodic minimum surface). A structure which is inspired us to study the impact strength of lightweight and high surface area of biomimetic Gyroid structure by the practice of additive manufacturing. Design parameters of Gyroid structure will be performed under UTM to study the load wearing capacity and mechanical behavior of deformed Gyroid. Deformed Gyroid structure under hydraulic compression give the data of stress strain curve so we can observe at what percent of strain lattice is deformed we will calculate deformed length with respect to compressive strength .We will also calculate the lattice volume and lattice density so we can observe at what volume and density lattice structure of Gyroid is deformed. The network phase gyroid is characterized by a continuous network of one type of polymer that is interconnected by channels of the other type of polymer.

Keyword: FDM, Bio mimics Lattice, Gyroid structure, TPMS, Compressive strength, ASA, Network phase gyroid

LIST OF ABBREVIATIONS

| | |
|----------------|--|
| ASA | Acrylonitrile styrene acrylate |
| AM | Additive manufacturing |
| ASTM | American Society for Testing and Materials |
| CAD | Computer-Aided Design |
| C | Celsius |
| cm | centimetre |
| FDM | Fused deposition modelling |
| g | gram |
| Hz | hertz |
| KN | kilo newton |
| Kpa | kilo Pascal |
| m ² | metre square |
| mm | millimetre |

| | |
|------|---------------------------------|
| 3d | three dimensional |
| STL | Standard Tessellation Language |
| TPMS | Triply periodic minimum surface |
| UV | Ultra violet |
| UTM | Universal testing machine |

1. INTRODUCTION

Bio mimetic is a bio inspired TPMS structure which is a regular lattice structure in which unit cell repeated in pattern like gyroid, primitive and diamond structures. TPMS structures have good surface to volume ratio and great connectivity of pore inside which makes good stiffness combination.

Gyroid structure was discovered in 1970 by a scientist alen schoen which having the mathematic trigonometric geometry. Gyroid infill pattern have the cubic geometry which is isotropic structure it means resistance is equally distributed for the forces that comes from all directions , so load bearing capacity of Gyroid is outstanding , infill of gyroid structure have good strength. Gyroid structure having the property of self-assembled periodic pattern with good mechanical and material behavior and light weight which we can use in automobile and aerospace industry .These kind of structures found in biological organisms like wings of butterfly and in the feathers of the birds, Since the mimicry of human bone is found in gyroid structure, So human bone transplant is done by these kind of structures which is very helpful in biomedical field.

In the recent years we have seen many applications of additive manufacturing. FDM is one of the AM technique in which polymer is used as filament and part is formed layer by layer as fuse deposition modeling biomimetic structure can printed by 3d printing, The mechanical behavior of gyroid porous structure with ASA filament will be studied, ASA is a Biodegradable polymer, which is not reactive with UV rays though it will increase the durability.

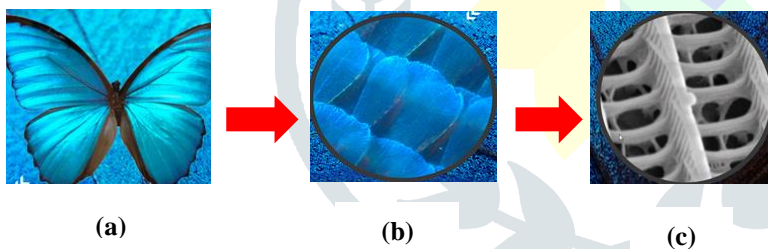


Fig. 1.1 (a) Butterfly (b) Close-up view of wings of butterfly (c) Bio mimetic porous lattice structure of butterfly wings

1.2 Gaps identified

- ❖ Testing of Design parameters and materials property of gyroid
- ❖ FDM with ASA filament
- ❖ Impact strength test of ASA printed Gyroid structure

1.3 Objectives of the project

The main objective of the project is to study the design parameters of formula based network phase gyroid lattices and to investigate the load varying capacity of filler and non-filler lattices.

2. MODELING AND METHODOLOGY

2.1 Modeling of Lattice structure

The gyroid structure is a type of mathematical construct that exhibits a repeating pattern of interconnected channels and surfaces forming a continuous, self-similar network. This has the mathematic trigonometric geometry.

$$\sin x \cos y + \sin y \cos z + \sin z \cos x = 0$$

Volumetric lattice gyroid structure is modeled in Autodesk fusion 360 software extension, Specimen is designed with the dimension 50mm*30mm*50mm. Gyroid is designed at following parameters.

- ❖ Solidity wall thickness
- ❖ Cell size
- ❖ Lattice transformation

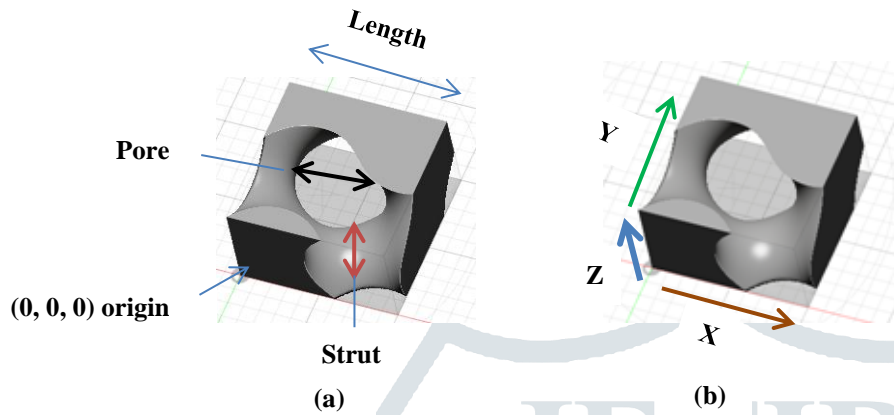


Fig.2.1 (a) Labeled unit cell of Gyroid (b) labeling of cell size in X, Y & Z direction

3x3x3 cell of gyroid structures are designed on the basis of three design parameters.

Table 2.1 Parameters of gyroid Type A

Type A Gyroid:

| Cell size (Uniform) | Solidity (Uniform) thickness | Lattice transform (orientation) |
|----------------------------------|------------------------------|--|
| X : 13mm Y : 13mm Z : 13mm | 0.35mm | Horizontal: X axis rotates 27° from origin. Vertical: Y axis rotates 25° from origin. |

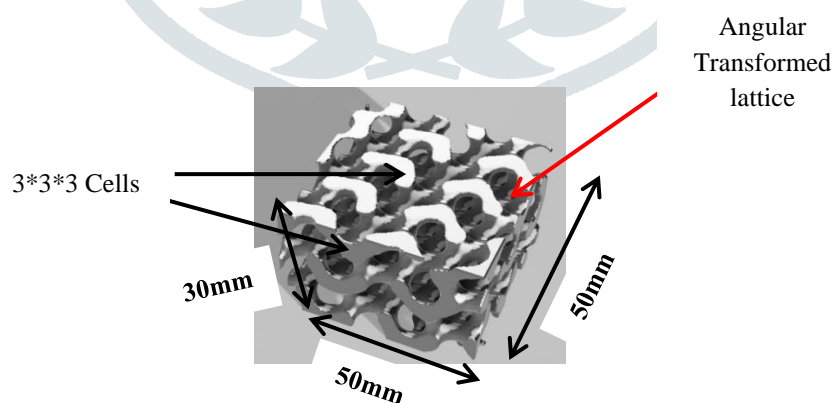


Fig.2.2 Shaded design of Type A gyroid, an isometric view

Table 2.2 Parameters of gyroid Type B

Type B Gyroid:

| Cell size (Non Uniform) | Solidity (Uniform) thickness | Lattice transform (orientation) |
|----------------------------------|------------------------------|---------------------------------|
| X : 20mm Y : 15mm Z : 10mm | 0.40mm | Not changed |

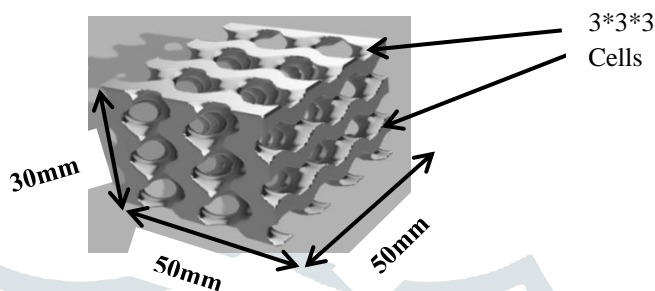


Fig.2.3 Shaded design of Type B gyroid, an isometric view

Table 2.3 Parameters of gyroid Type C

Type C Gyroid:

| Cell size (Non Uniform) | Solidity (Uniform) thickness | Lattice transform (orientation) |
|----------------------------------|------------------------------|---------------------------------|
| X : 20mm Y : 15mm Z : 10mm | 0.35mm | Not changed |

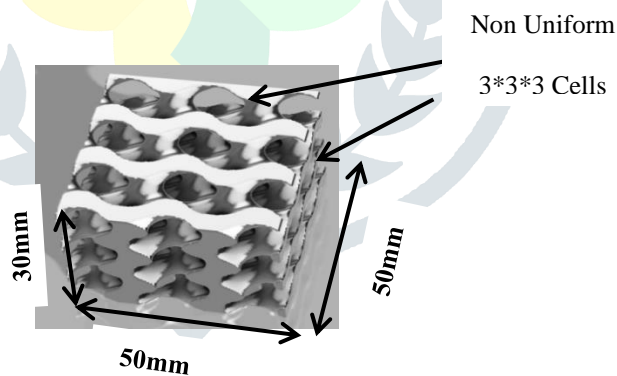


Fig.2.4 Shaded design of Type C gyroid, an isometric view

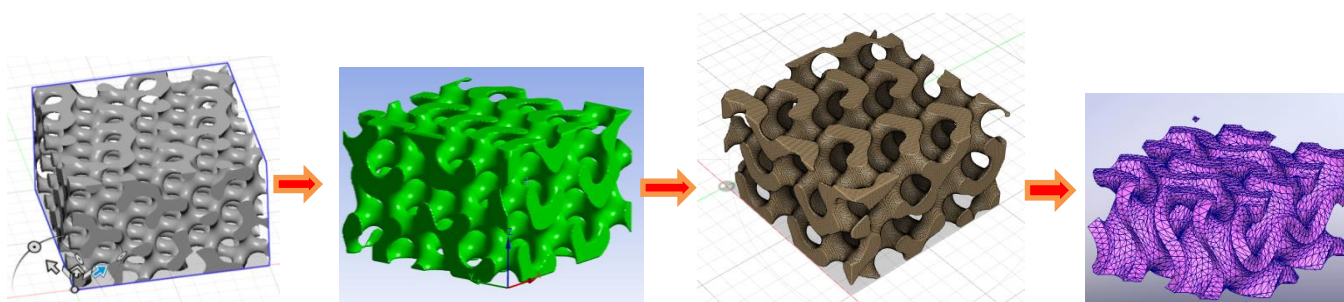


Fig.2.5 (a) Cad design

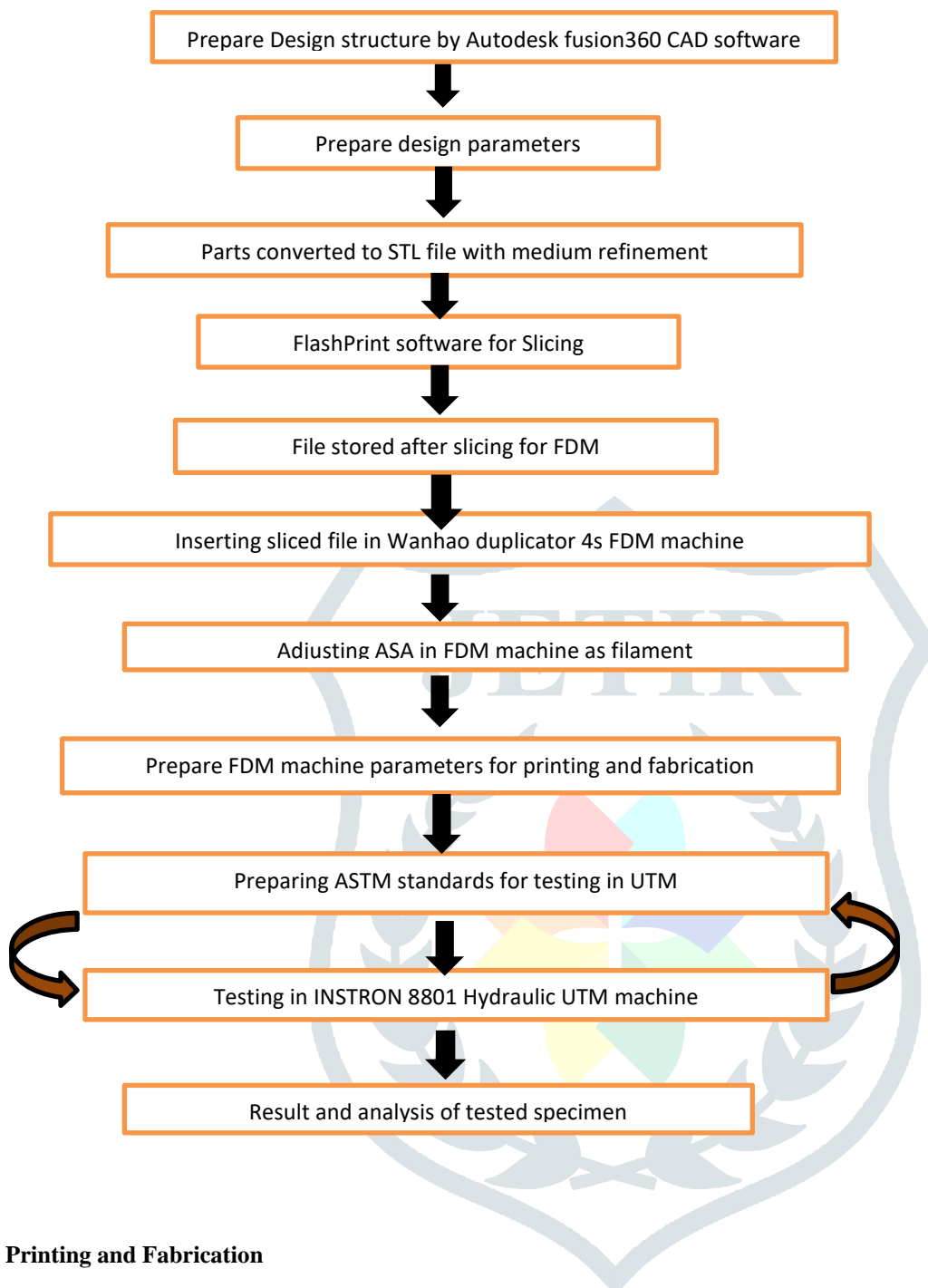
Fig.2.5 (b) Shaded design

Fig.2.5 (c) Wireframe shaded design

Fig.2.5 (d) Mesh structure

Fig.2.5 Optimized design of gyroid structure

2.2 METHODOLOGY



2.3 Printing and Fabrication

FDM (Fused deposition modeling) technique of additive manufacturing is used for the printing of strut based Gyroid structure. ASA (Acrylonitrile Styrene Acrylate) filament is used for fused filament fabrication. ASA filament wire having diameter of 1.75mm

FDM machine named Wanhao Duplicator 4s is used for 3d printing which having nozzle diameter of 0.40mm. STL file created for the FDM printing having mesh size of 0.329 mm with medium refinement. File was sliced through the FlashPrint software in which infill density 100% and infill pattern triangle is used. In slicing layer height fixed first layer height 0.30mm and then 0.20mm .Printing speed and travel speed fixed of 60mm/sec and 80mm/sec respectively. Printing temperature fixed in slicing extruder temperature 245 C and platform temperature 100 C is used.

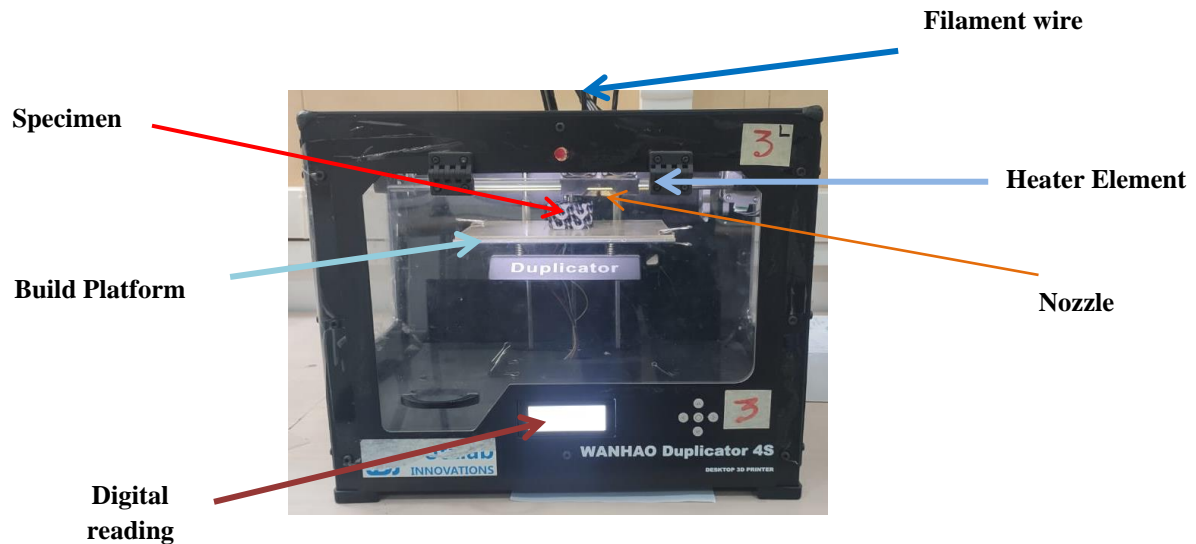


Fig. 2.6 A schematic view of FDM machine

Total 9 specimens, 3 parts of each type of Gyroid were printed. 5 h 10m was the Average printing time recorded and 10.15m avg filament were used in each part of specimen in FDM printing.



Fig. 2.7 (a)

Fig. 2.7 (b)

Fig. 2.7 (c)

Fig. 2.7 A biomimetic structure of TPMS FDM printed Gyroid (a) Top view of specimen (b) Isometric view of specimen (c) Side view of specimen

3. EXPERIMENTAL METHODS

3.1 Quasi-static flatwise compression tests:

The term "quasi-static" refers to the fact that the compression is applied slowly enough that the material's response can be assumed to be quasi-static or quasi-equilibrium, meaning that its properties remain constant throughout the test and material is subjected to compressive force very slow.

Quasi-static test perform by using INSTRON 8801 hydraulic universal testing machine with loading rate of 2mm/min, which is controllable test was performed at 26-degree room temperature and humidity was 60%. The mechanical properties of lattice structure of Gyroid experienced in quasi-static process, an axial load applied gradually initially from 3KN in UTM .The ASA printed porous structure was sandwiched between two plates of steel. A Total 9 deformation test were performed All 3 parts of each type Gyroid were tested on UTM machine. So we can study the accurate result of load displacement curve. The load-displacement curve was

measured by transducer of UTM machine at 1000 Hz frequency. The deformation images were captured by smartphone camera throughout the quasi-static process.

3.2 ASTM standard Testing

ASTM C365 was used for flatwise compression test in which specimen sandwiched and axial load applied for computing the compressive strength and effective modulus of specimen. Compressive stress at maximum load and strain at maximum load can observe in the form of displacement curve.

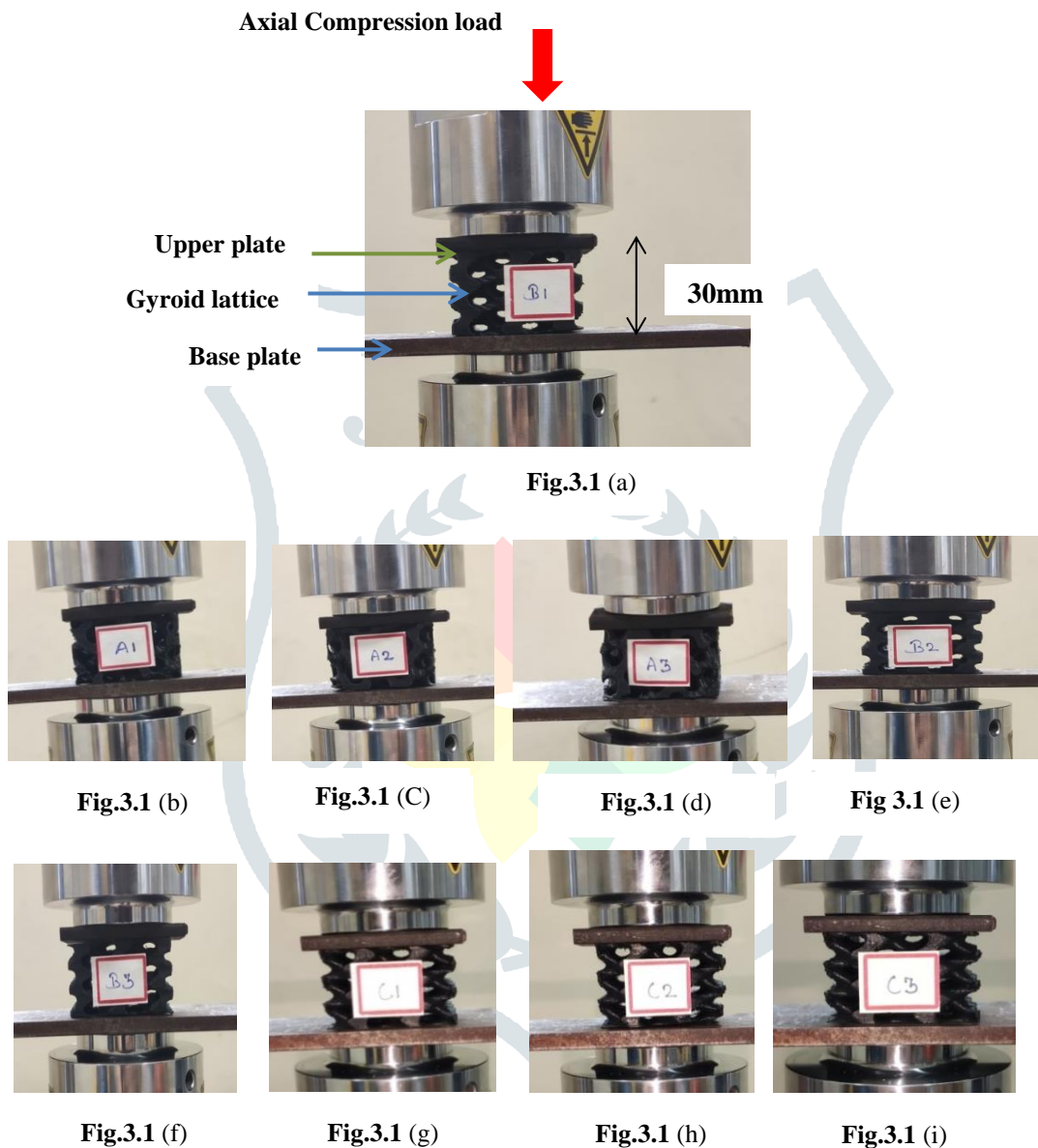


Fig. 3.1 Compression testing of specimens on the basis of ASTM standards

3.3 Stress-strain curve

Stress-strain curve is the study of mechanical properties of deformed material, where as compressive stress is the applied load which is responsible for the deformed lattice body, with respect of decreasing volume. Compressive strain is the deformation of length with respect of applied force in axial direction.

Stress-strain curve is the graph plotted between compressive stress and compressive strain to study the elastic limit and relationship between stress and strain under different loads to observe the mechanical behaviour of material.

Elastic region:

Following the fig(a) There is elastic region of 0 to 11% , which obeys hooks law of proportion limit where we can find the stress strain ratio as proportionality constant known as young’s modulus and elastic limit beyond that limit the material will not able to reform its original position.

Plastic region:

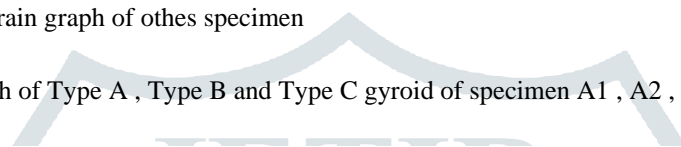
Following the fig(a) the plastic deformation will be occur in plastic region between compressive strain 11 to 22% , In plastic region body will be attain maximum yield point where body fall in permanent plastic deformation and material will be achieve maximum ultimate stress before the failure.

Failure region:

The fracture and breaking point where failure of material takes place. We can see in the fig. (a) curves goes down at 3.5kpa compressive stress and 22% of compressive strain which is th failure region.

Same we can follows the stress-strain graph of othes specimen

Following is the stress-strain graph of Type A , Type B and Type C gyroid of specimen A1 , A2 , A3 , B1 , B2 ,B3 and C1 , C2 , C3.



Graph 1

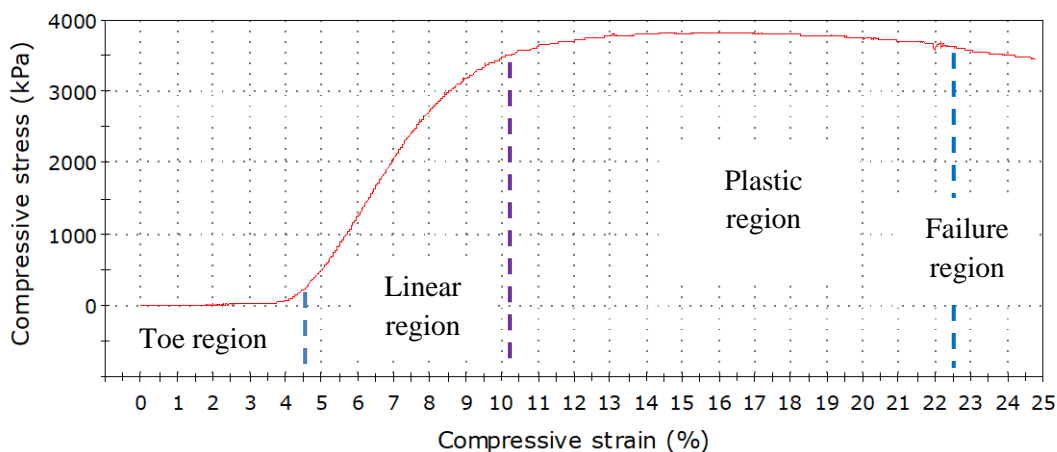


Fig. 3.2 (a) stress-strain graph of A1 specimen

Graph 1

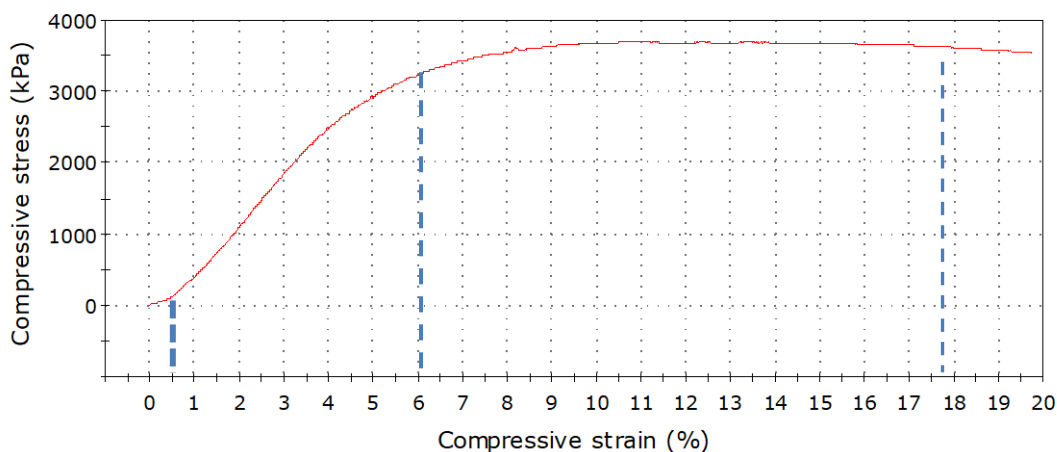


Fig. 3.2 (b) stress-strain graph of A2 specimen

Graph 1

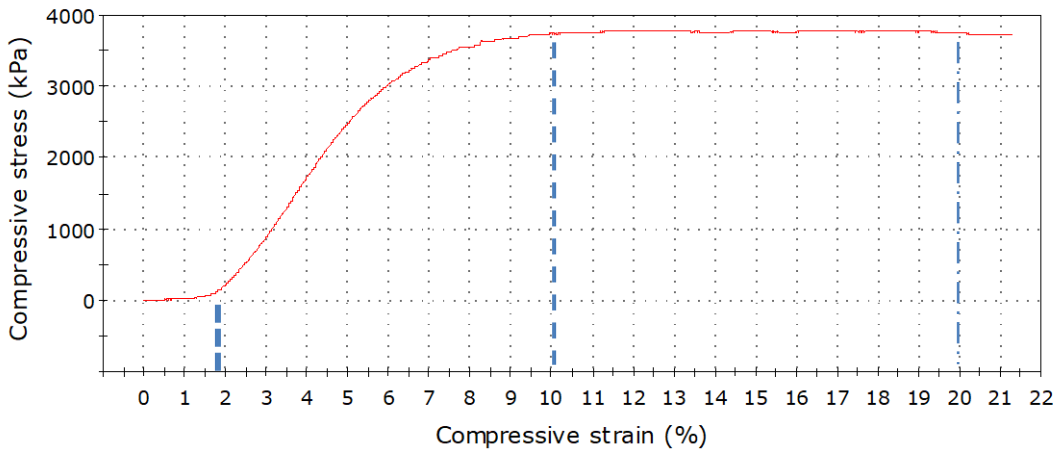


Fig. 3.2 (c) stress-strain graph of A3 specimen

Graph 1

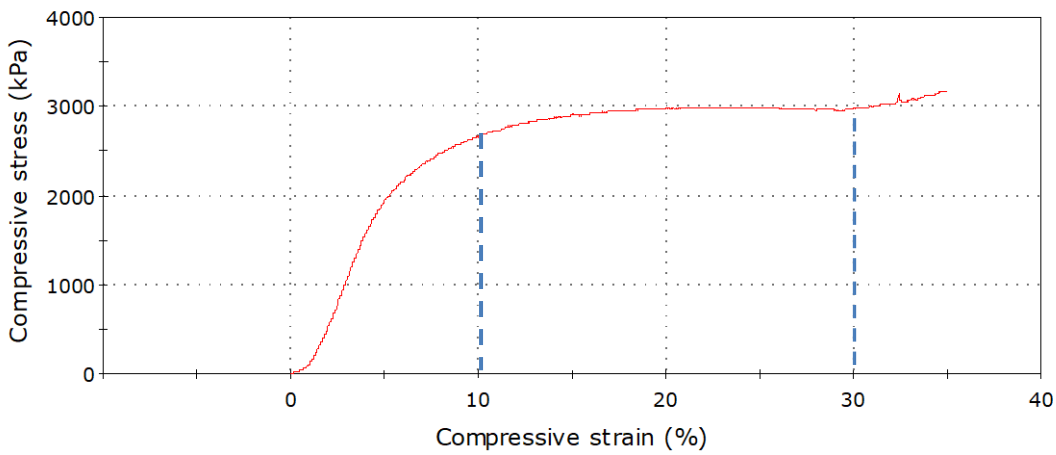


Fig. 3.2 (d) stress-strain graph of B1 specimen

Graph 1

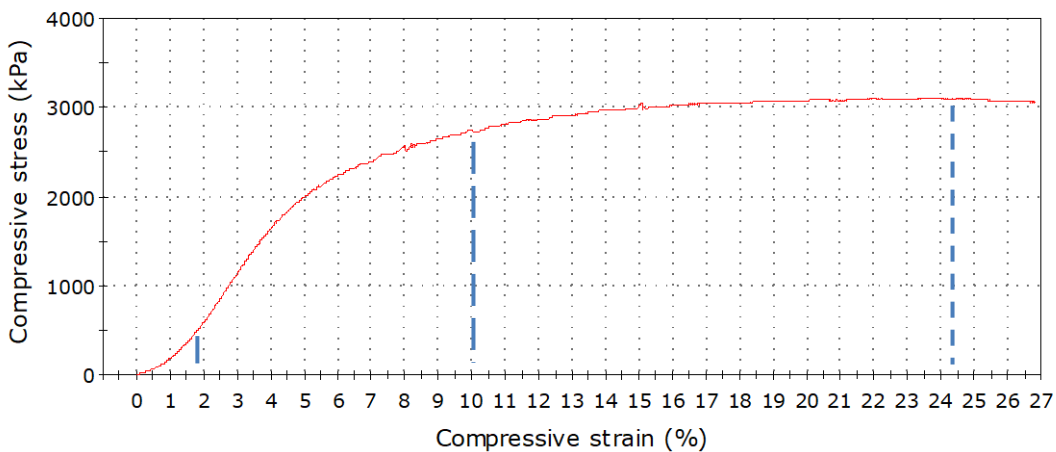


Fig. 3.2 (e) stress-strain graph of B2 specimen

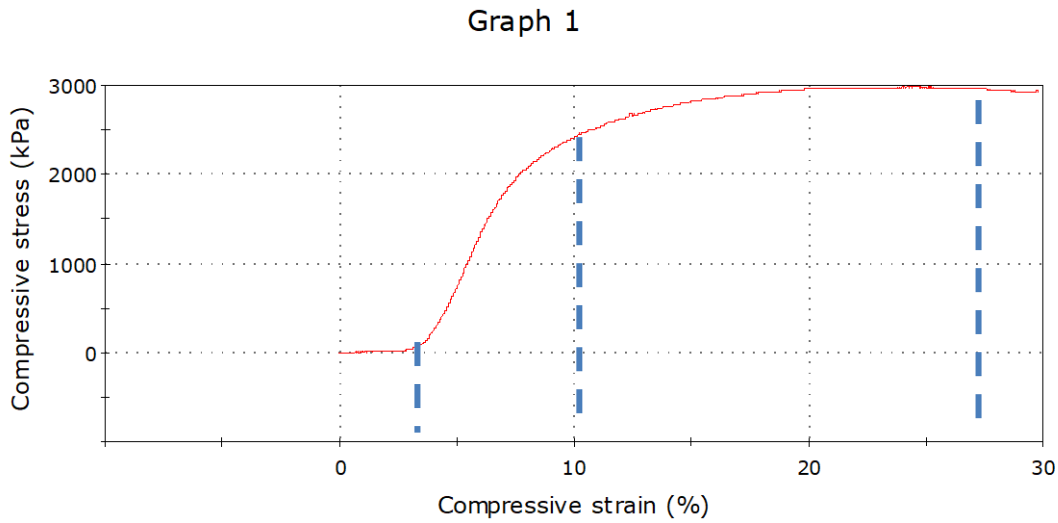


Fig. 3.2 (f) stress-strain graph of B3 specimen

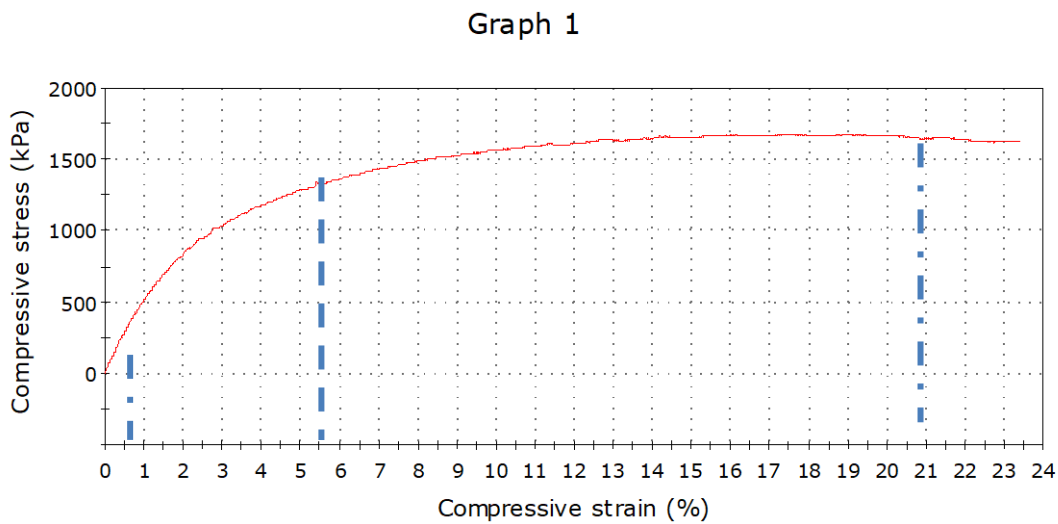


Fig. 3.2 (g) stress-strain graph of C1 specimen

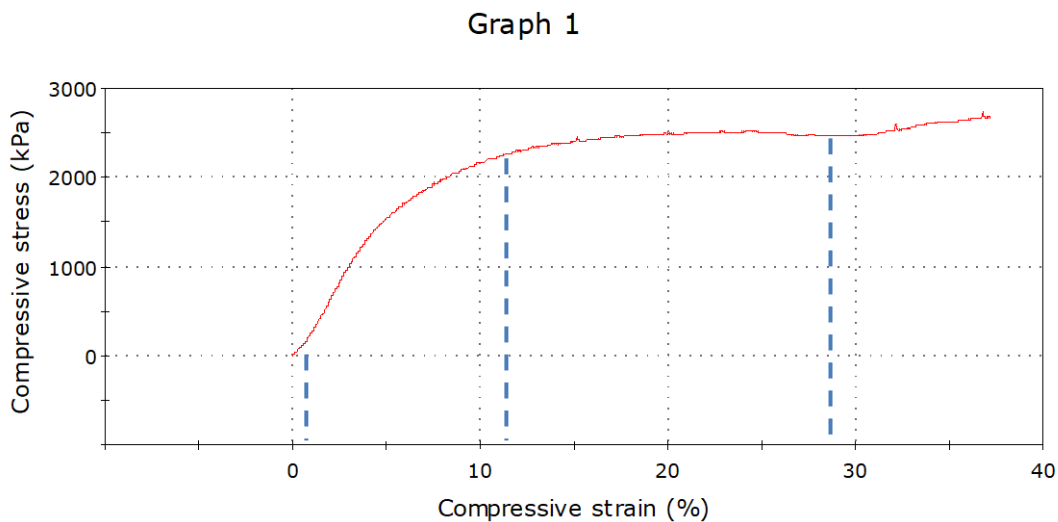


Fig. 3.2. (h) stress-strain graph of C2 specimen

Graph 1

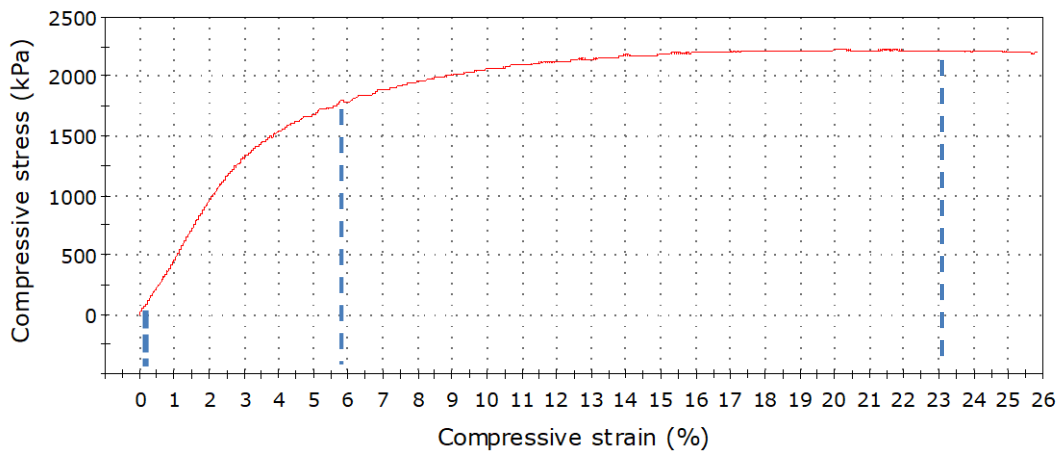


Fig 3.2 (i) stress-strain graph of C3 specimen

Fig.3.2 Stress-strain graph of all experimented specimens

3.4 Property of gyroid structure with fillers

A gyroid structure with fillers refers to a type of composite material that consists of a porous, three dimensional network with a gyroid structure that is filled with a second material. The filler material is typically added to the gyroid structure to enhance its mechanical properties, such as stiffness, strength and toughness. The choice of filler material depends on the desired properties of the composite, as well as the processing method use to fabricate it. For example filler such as carbon nanotube, graphene or ceramic particles may be added to improve the strength or thermal properties of the composite.



Fig. 3.3 (a)



Fig. 3.3 (b)

In the above images the structure have been filled with silicone paste. A silicone is a polymer made up of siloxane which after cured act like a rubber, which having the property of low thermal conductivity, thermal stability with constancy of temperature -100 to 250 C, low chemical reactivity and low toxicity.

3.5 Fractured of gyroid under quasistatic load

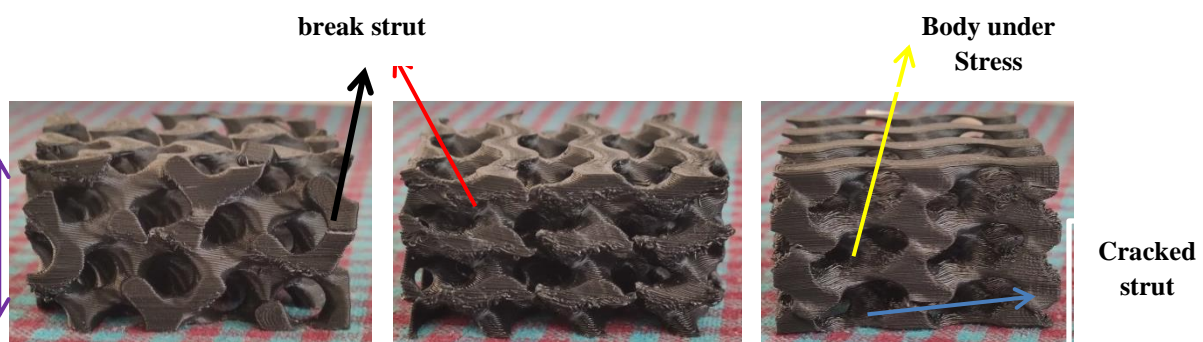


Fig.3.4 (a) Side view of fractured specimen Type A

Fig.3.4 (b) Side view of fractured specimen Type B

Fig.3.4 (c) Side view of fractured specimen Type C

Fig.3.4 Fractured view of gyroid after compression tests

In the above figure it is shown that the specimens is fractured and break at different percentage of strain in the process of quasi static load the wall structure is crack and the alignment of wall structure is break because strut of gyroid is break we can see the stress mark in body , the deformation of strcture changes the length of gyroid which we can calculate in the caculation.Since body of strcture is getting shrinked after compression so the diameter and size of the cell is also effected , as a result of quasi static axial load the strut of gyroid is break at maximum stress.

3.6 Simulation analysis of gyroid structure

The matrix phase gyroid is characterized by a continuous matrix of one type of polymer that is filled with a network of channels, the pattern of cells is repeated in the interconne ted network.

Design has been optimised in the software parameter , CAD design has been developed Convereted into the mesh structure , the mass and energy of body part hab been divided into small elements so we can analyse the body by computational methods.

Simulation is done on software , where the geometry of gyroid is fixed in base and axial load was applied on the top of geometry . The 2*2*2 cell of matrix phase gyroid having dimension of 20mm*20mm*20mm is deformed by giving the 1 KN load we can see the deformed structure gives the data of von mises stress, strain and displacement as result of simulation .

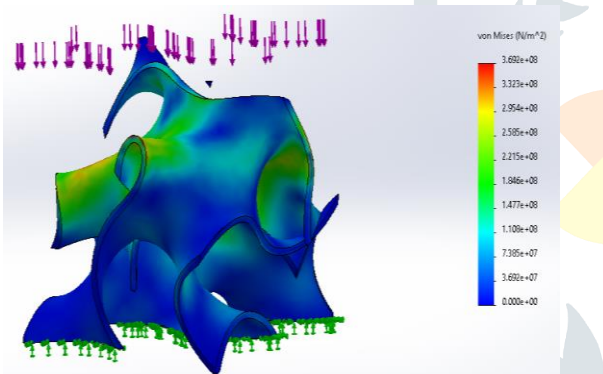


Fig.3.5 (a) VonMises stress

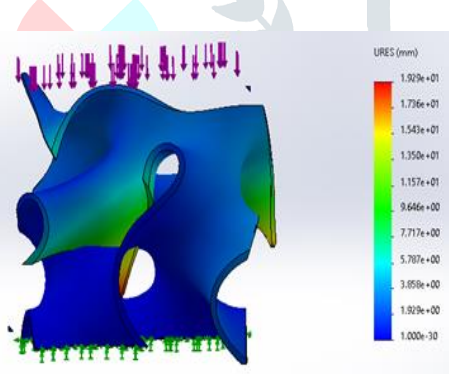


Fig.3.5 (b) Displacement

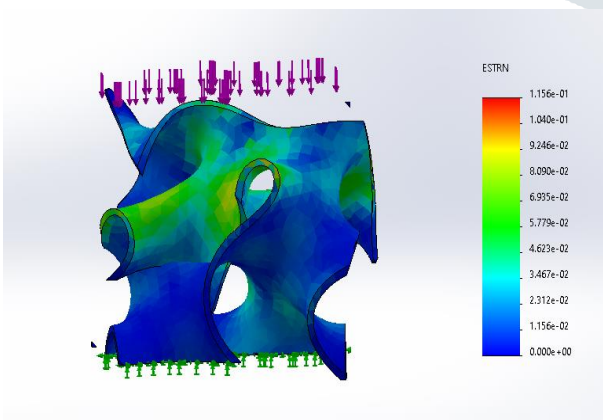


Fig.3.5 (c) VonMises strain

Fig. 3.5 Simulation images of matrix phase gyroid

In the above fig. we can see how the axial compressive load effect material of the body , the data of deformed body is also included in the above figures

4. RESULTS AND CALCULATIONS

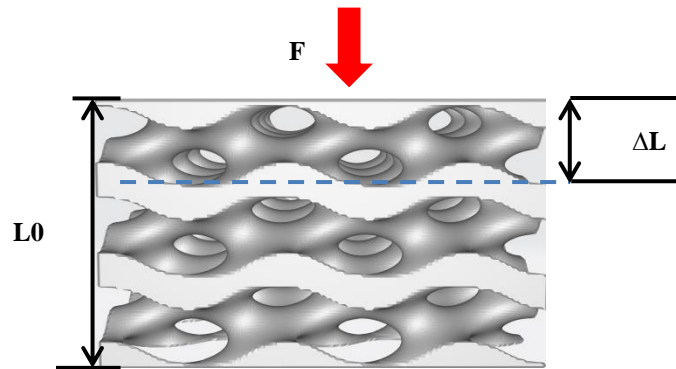


Fig.4.1 Compression of Gyroid with deformation of ΔL

4.1 Calculations:

According to the Hooke’s formula stress is directly proportional to strain, so we can calculate the change in length of deformed Gyroid

$$\sigma = \gamma \times \epsilon$$

Where σ = stress, ϵ = strain, γ = Young’s modulus of elasticity

$$\text{Stress } (\sigma) = \frac{\text{Axial compressive load (F)}}{\text{Surface area of gyroid (A)}}$$

$$\text{Strain } (\epsilon) = \frac{\text{Change in length } (\Delta L)}{\text{Original length } (L_0)}$$

Where A = 2500 mm², L₀ = 30 mm

$$\Delta L = \frac{1}{\gamma} \frac{F L_0}{A}$$

By the above equation we can calculate the deformed length of gyroid lattice where F is the quasi-static load applied axially.

Table 4.1: Observation table of effected length with respect to the compressive load and elasticity

| S.No. | Specimen label | Maximum Compression load(F) in N | Compressive strength(F/A) in N/mm ² | Young’s Modulus of elasticity (γ) in N/mm ² | Change in length ΔL in mm | Effected length L= L ₀ -ΔL, L ₀ =30 in mm |
|-------|----------------|----------------------------------|--|--|---------------------------|---|
| 1 | A1 | 9583.30664 | 3.83332 | 79.41606 | 1.447 | 28.553 |
| 2 | A2 | 9249.70508 | 3.69988 | 71.25583 | 1.557 | 28.443 |
| 3 | A3 | 9460.26465 | 3.78411 | 83.40590 | 1.361 | 28.639 |
| 4 | B1 | 7921.03418 | 3.16841 | 49.57306 | 1.917 | 28.083 |
| 5 | B2 | 7751.84033 | 3.10074 | 47.18720 | 1.970 | 28.030 |
| 6 | B3 | 7436.13232 | 2.97445 | 50.00320 | 1.784 | 28.216 |
| 7 | C1 | 4186.17139 | 1.67447 | 37.16973 | 1.351 | 28.649 |

| | | | | | | |
|------|----|------------|---------|----------|-------|--------|
| 8 | C2 | 6851.83984 | 2.74074 | 35.21303 | 2.334 | 27.666 |
| 9 | C3 | 5581.80225 | 2.23272 | 44.56707 | 1.502 | 28.498 |
| mean | | 7558.01074 | 3.02320 | 55.31012 | 1.691 | 28.308 |

Calculation of Lattice density:

Density which is the ratio of weight and volume, all 9 specimens' weight measured in weighing machine, whereas volume of gyroid lattice was captured through the software.



Fig.4.2 B1 specimen weight in weighing machine

$$\text{Density } (\rho) = \frac{m \text{ (weight of weighed gyroid)}}{V \text{ (volume of lattice structure)}}$$

$$\text{Volume fraction (V \%)} = \frac{\text{Lattice Volume} \times 100}{\text{Volume of solid body}}$$

Whereas volume of solid body = 75000 mm², weight of solid body without infill structure is = 79g

$$\text{Density of solid body} = \frac{79}{75000} = 0.00106\text{g/mm}^3$$

$$\text{Infill density } (\rho \%) = \frac{\text{Lattice density} \times 100}{\text{Density of solid body}}$$

Table 4.2: Observation table of lattice density with respect to the lattice volume and weight of gyroid

| S. No. | Specimen label | Lattice volume(V) in mm ³ | V % | Weight(m) of specimens (g) | Lattice density (ρ) in g/mm ³ | Infill density ρ % |
|--------|----------------|--------------------------------------|-------|----------------------------|--|--------------------|
| 1 | A1 | 26476.389 | 35.30 | 22.92 | 0.000865 | 81.60 |
| 2 | A2 | 26476.389 | 35.30 | 22.78 | 0.000860 | 81.12 |
| 3 | A3 | 26476.389 | 35.30 | 22.94 | 0.000866 | 81.69 |
| 4 | B1 | 30361.458 | 40.48 | 24.56 | 0.000808 | 76.22 |
| 5 | B2 | 30361.458 | 40.48 | 24.65 | 0.000811 | 76.50 |
| 6 | B3 | 30361.458 | 40.48 | 24.28 | 0.000799 | 75.37 |
| 7 | C1 | 26942.708 | 35.92 | 21.28 | 0.000789 | 74.43 |
| 8 | C2 | 26942.708 | 35.92 | 21.90 | 0.000812 | 76.60 |
| 9 | C3 | 26942.708 | 35.92 | 21.40 | 0.000794 | 74.90 |

Table 4.3: Observation table of lattice mean density with respect to the lattice volume and weight of gyroid

| S. No. | Specimen | Mean lattice volume V % | Mean weight of specimen | Mean weight of infill density ρ % |
|--------|----------|-------------------------|-------------------------|--|
| 1 | Type A | 35.30 | 22.88 | 81.47 |
| 2 | Type B | 40.48 | 24.49 | 76.03 |
| 3 | Type C | 35.92 | 21.52 | 75.31 |

5. CONCLUSION

The results shows the lattice-transformed Gyroid which has lattice transformation in the vertical and horizontal direction by giving the angle of geometry $x = 25^\circ$ and $y = 27^\circ$, the performance has been increased elastic modulus, compression test and energy absorption at 25 % strain the failure region is between 25% to 30%.

The mechanical property was changed with changing the angular geometry the infill density was increased with mean density ρ % of 81.47 %. The lattice volume of type A Gyroid was also min. compared to other Gyroid structures with mean V % of 35.30 as result the mean weight of lattice Gyroid was 22.88g which was less compared to the other Gyroid. It means the result of the compression test shows that geometrically angular transformed Gyroid can absorb more weight compared to the regular TPMS Gyroid which has different design parameters. The shape of lattice structure can change by adjusting the angles the relative density and performance can also be predicted to meet certain requirements. Gyroid structures with fillers have potential applications in various fields, including aerospace, automotive, and biomedical for example gyroid composites can be used as a lightweight structural material for aircraft and spacecraft components. The unique geometry of the gyroid structures also offers interesting opportunities for applications in photonics, sensing, and catalysis.

5.1 Observations: Following are the important observations throughout my project.

- ✓ Nozzle diameter varies with the material.
- ✓ Nozzle diameter can affect the layer height and path width.
- ✓ 0.4 mm nozzle diameter can achieve accuracy up to 100 micron.
- ✓ Printing time decreases with increasing nozzle diameter vice-versa.
- ✓ Temperature does not affect the thermochemical properties of ASA.
- ✓ Surface roughness causes by the stair case effect, which is visible in curved surfaces.
- ✓ Factors affecting the compressive strength of gyroid
 - ❖ Lattice transformation
 - ❖ Volume of lattice structure
 - ❖ Infill density of lattice

6. ACKNOWLEDGEMENT

I would like to express my extreme sincere gratitude and appreciation to my guide Dr. Aravind Raj S, Professor in the department of manufacturing engineering and faculty of sustainable manufacturing, Vellore institute of technology for his creative and comprehensive guidance until this project come to existence.

I would like to express my extreme sincere gratitude and appreciation to PHD scholar Shakti balan department of manufacturing engineering, Vellore institute of technology for his kind endless help, generous advice during my experiments and in my project work.

I am thankful to the lab In-charge of additive manufacturing lab, Department of manufacturing engineering for giving me permission to fabricate the part in the Additive manufacturing Lab facility.

I am thankful to the lab In-charge of advanced materials testing lab, department of manufacturing engineering for giving me permission to compression testing in advanced material testing lab facility.

7. REFERENCES

1. El Jai M, Herrou B, Benazza H (2013) Integration of a risk analysis method with holonic approach in an isoarchic context. *Int Eng. Technol* 5
2. El Jai M, Akhrif I, Herrou B, Benazza H (2015) Correction of the production master plan according to preventive maintenance constraints and equipment's degradation state. *Engineering* 6:274–291.
3. Wortmann, M.; Frese, N.; Brikmann, J.; Ehrmann, A.; Moritzer, E.; Hüsgen, B. Silicone mold accuracy in polyurethane vacuum casting. *Macromol. Symp.* 2021, 395, 2000242. [Han, S.H.; Cha, M.; Jin, Y.Z.; Lee, K.M.; Lee, J.H. BMP-2 and hMSC dual delivery onto 3D printed PLA-Bio gel scaffold for critical-size bone defect regeneration in rabbit tibia. *Biomed. Mater.* 2021, 16, 015019.
4. Aimar, A., Palermo, A., Innocenti, B., 2019b. The role of 3D printing in medical applications: a state of the art. vol. 2019, Article ID 5340616, 10 pages
5. Abueidda, D. W.; Elhebeary, M. Shiang Ch-S.; et al.; Mechanical properties of 3D printed polymeric Gyroid cellular structures: Experimental and finite element study. *Materials & Design* 165, 219,
6. Deepa Y 2014 A Rapid prototyping technique for product cycle time reduction cost effectively in aerospace applications, e-ISSN: 2278-1684, p-2320-334X, pp.62-68.
7. Schoen A H 1970. Infinite periodic minimal surface without self-intersections, Electronics Research Center Cambridge, Mass. 02139
8. Kooistra G W, Vikram V S and Wadley H N G 2004. Compressive behaviour of age hardenable tetrahedral lattice truss structures made from aluminium. *Acta Materialia* 52, pp. 4229-4237.
9. Williams C B, Allen J K, Rosen D W and Mistree F 2005. Process parameter platform design to manage workstation capacity, *Prod. Platform & Prod. Family Design: Methods and Applic.*, Eds.:
10. Gorguluarslan, R. M.; Park, S.; Rosen, D.; et al. A Multilevel Upscaling Method for Material Characterization of Additively Manufactured Part Under Uncertainties. *J. Mech. Des.* 2015, 137, 1 – 12.
11. Mizuno, A.; Shuku, Y.; Awaga, K.; Recent Developments in Molecular Spin Gyroid Research. *Bull. Chem. Soc. Jpn.* 2019, 92, 1068 – 1093